Supplementary figures

Melanoma exosomes educate bone marrow progenitor cells toward a pro-metastatic phenotype through MET

Héctor Peinado, Maša Alečković, Simon Lavotshkin, Irina Matei, Bruno Costa-Silva, Gema Moreno-Bueno, Marta Hergueta-Redondo, Caitlin Williams, Guillermo García-Santos, Ayuko Nitadori-Hoshino, Caitlin Hoffman, Karen Badal, Benjamin A. Garcia, Margaret K. Callahan, Jianda Yuan, Vilma R. Martins, Johan Skog, Rosandra N. Kaplan, Mary S. Brady, Jedd D. Wolchok, Paul B. Chapman, Yibin Kang, Jacqueline Bromberg, David Lyden

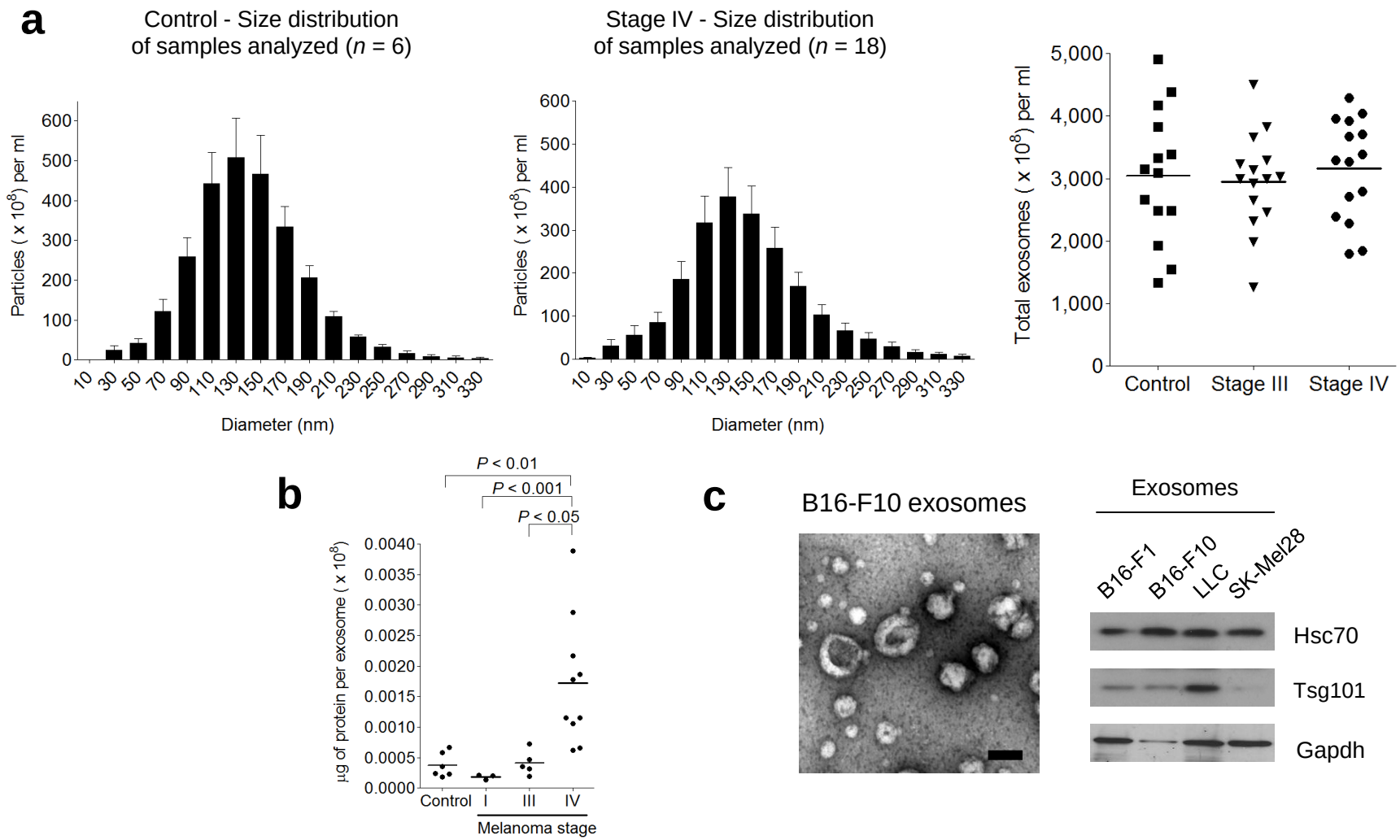

Supplementary Figure 1. Characterization of human circulating exosomes. Exosomes isolated from fresh plasma derived from healthy controls and melanoma subjects were measured by Nanoparticle Tracking Analysis (NanoSight). **(a)** Analysis of the size distribution (left and middle panels) and total circulating exosomes (right panel) in the plasma of healthy donors and melanoma subjects. The results are presented as the total number of particles (× 10^8) per milliliter of plasma. Error bars represent s.e.m. **(b)** Analysis of the protein content per exosome in circulating exosomes measured in human fresh plasma from healthy donors and Stage I, III and IV melanoma subjects. The results are represented as the total micrograms of protein divided by the total number of exosomes (× 10^8) measured by NanoSight. **(c)** Representative electron microscopy imaging of exosomes derived from B16-F10 melanoma cells in culture (Bar = 100 nm) (left panel). Representative Western blot analysis of exosome markers (Hsc70 and Tsg101) in exosomes isolated from the supernatant fraction of B16-F1, B16-F10, LLC and SK-Mel28 cell lines (right panel). Gapdh was used as loading control.

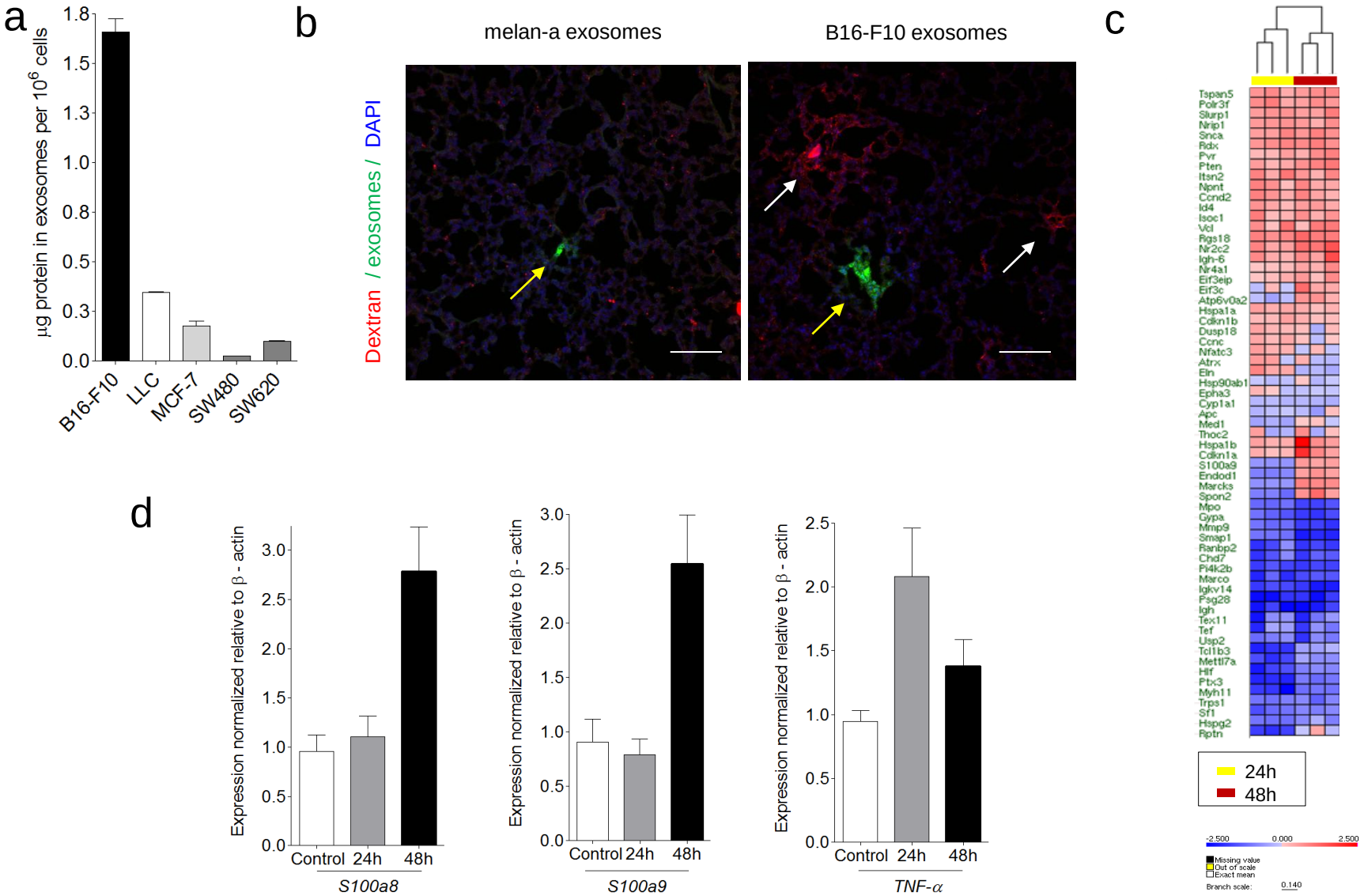

Supplementary Figure 2. Exosome effects in metastatic organs. (a) Measurement of the total protein per million cells in the exosomes isolated from low metastatic mouse lung cancer (LLC), human breast cancer (MCF-7), and human colon cancer cells (SW480 and SW620) compared to highly metastatic B16-F10 mouse melanoma cells in culture. Error bars represent s.e.m. **(b)** Analysis of lung vessel leakiness 24 h after tail vein injection of 10 µg of melan-a or B16-F10 exosomes. Yellow arrow: green labeled exosomes. White arrow: red dextran = endothelial leakiness area (Scale bar = 100 µm) **(c)** Microarray cluster analysis of genes differentially expressed in the lungs 24 and 48 h after tail vein injection of 10 µg of B16-F10 exosomes compared to control (see **Supplementary Table 3** for a detailed list of the genes) **(d)** QRT-PCR analysis of indicated genes from RNA isolated from lungs 24 and 48 h after tail vein injection of 10 µg B16-F10 exosomes .

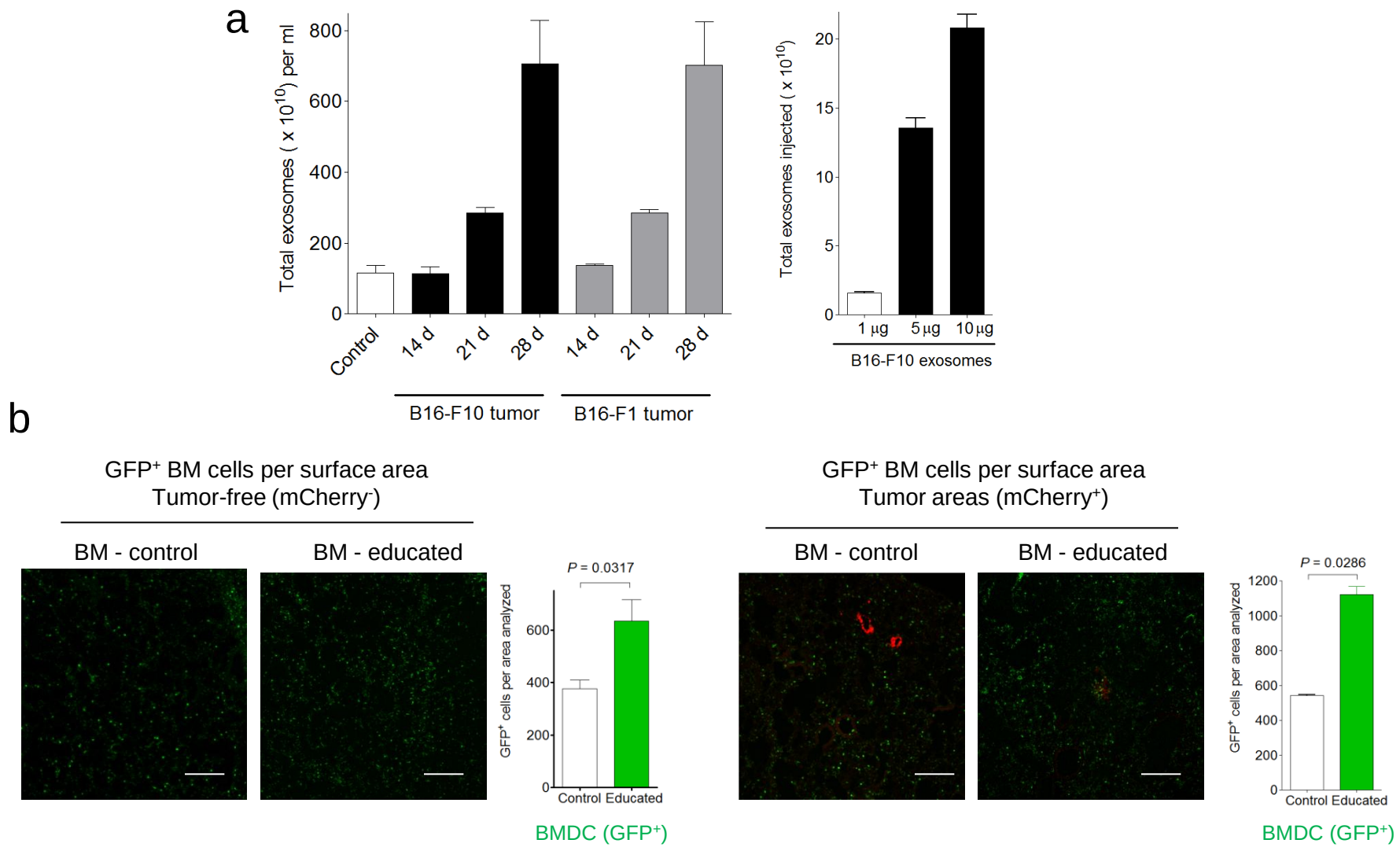

Supplementary Figure 3. Analysis of circulating exosomes and BMDC infiltration during lung metastasis after BM education. (a) Characterization of total circulating exosome levels in the plasma of control mice or mice bearing day 14, 21 and 28 B16-F10 and B16-F1 tumors (left graph). The results are presented as the total number of exosomes (× 10^{10}) per milliliter of plasma. NanoSight analysis of total tumor exosomes injected in mice for BM education experiments (right graph). Results are presented as the total number of exosomes (× 10^{10}) per injection of 1, 5 and 10 μg exosomes. Error bars represent s.e.m. **(b)** Confocal microscopy analysis of BMDCs (GFP-green) in lungs from BM-educated mice and controls (scale bar = 50 μm). Quantification of total BMDCs per confocal field analyzed in tumor-free areas (left panel) or areas with metastases (mCherry$^+$, right panel) is shown in the green graphs (n = 5 mice per group; error bars represent s.e.m).

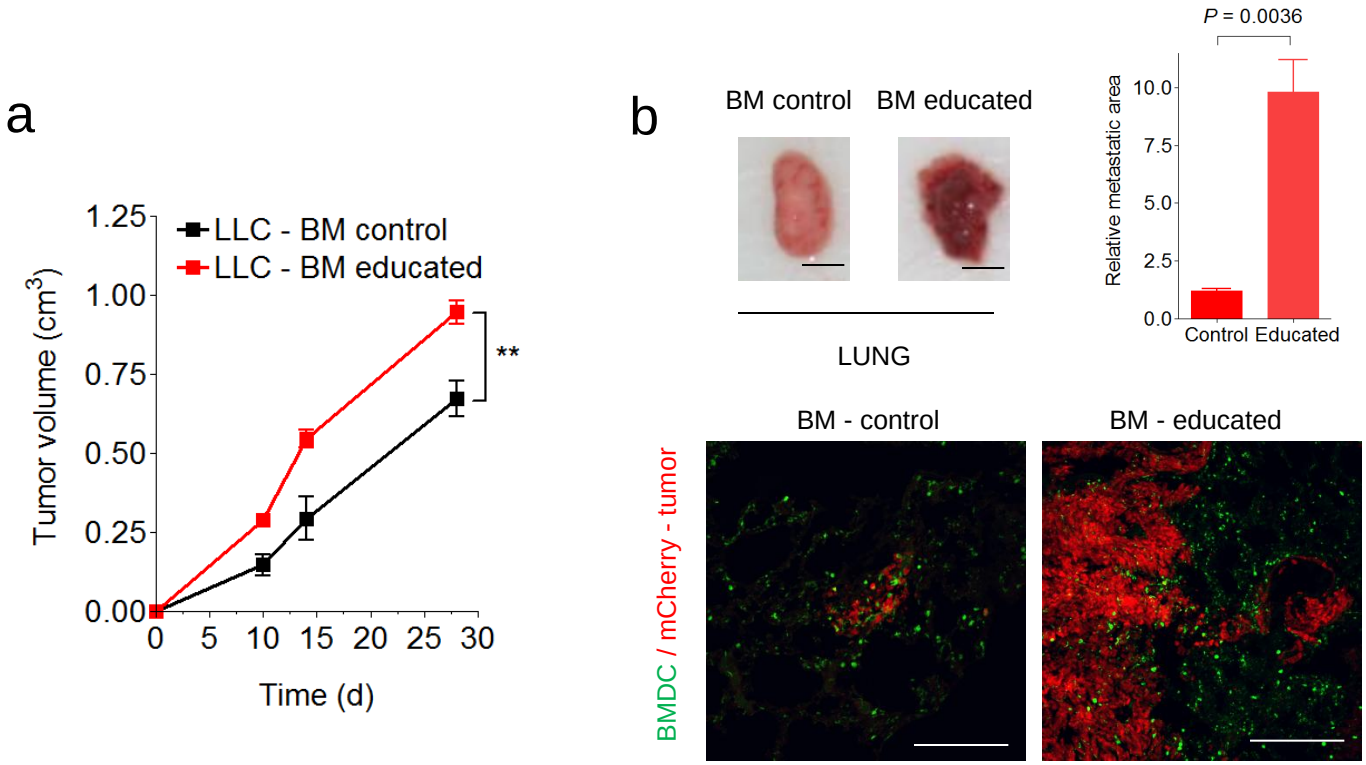

Supplementary Figure 4. Analysis of primary tumor growth after subcutaneous flank injection of LLC cells. (a) Analysis of primary tumor growth after subcutaneous flank injection of LLCmCherry tumor cells in mice transplanted with B16-F10 exosome-educated BM (BM educated). BM derived from mice treated with control particles (BM-control) and PBS (not shown) was used in parallel (n = 5 mice per group; error bars represent s.e.m.; $^{**}P < 0.01$ by ANOVA). **(b)** Representative picture of macroscopic lung metastases (upper left panel, black bar = 200 mm). Representative picture of LLCmCherry metastases after 28 d of B16-F10-exosome BM education (lower panels, scale bar = 50 μm). Quantification of the metastatic area relative to control (red graph; right panel, top; n = 5 mice per group; error bars represent s.e.m).

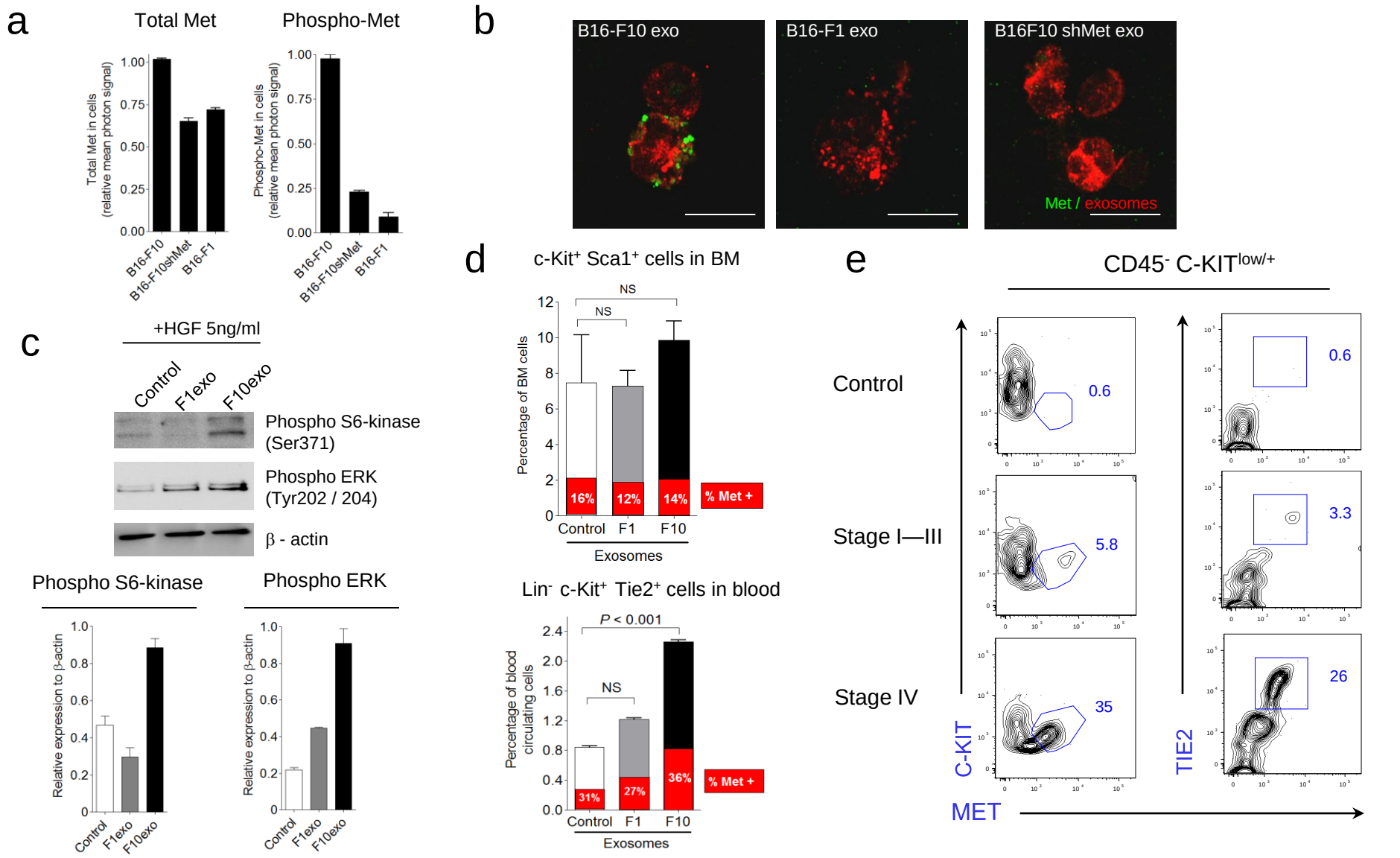

Supplementary Figure 5. Analysis of Met expression in melanoma and BM cells. (a) Analysis of Met and phospho-Met expression in B16-F10, B16-F1, cells and B16-F10shMet cells. **(b)** Immunofluorescence analysis of the horizontal transfer of Met to BM cells after overnight treatment with 20 μg ml^{-1} of B16-F10, B16-F10shMET, and B16-F1 exosomes (exosomes labeled in red, Met in green, scale bar = 20 μm). **(c)** Western blot analysis of phospho-S6 kinase and phospho-ERK in BM cells pre-treated with 20 μg ml^{-1} of B16-F10 and B16-F1 exosomes for 16 h and then stimulated with HGF (5 ng ml^{-1}) for 4 h. β-actin was used as loading control and quantification is shown below. **(d)** Flow cytometric analysis of Met expression in c-Kit^+Sca1^+ cells in BM (upper panel) or Lin^-c-Kit^+Sca1^+ circulating BM cells in blood (lower panel) of control mice and mice educated with 10 μg of B16-F10 or B16-F1 exosomes every other day for 28 . Red area = percentage of Met^+ cells. Error bars represent s.e.m.; NS = not significant; $P < 0.001$ by ANOVA. **(e)** Representative flow cytometric analysis of MET expression in circulating BM progenitor cells ($CD45^-$C-$KIT^{low/+}$ and $CD45^-$C-$KIT^{low/+}TIE2^+$) from the blood of Stage I—III and IV melanoma and control subjects.

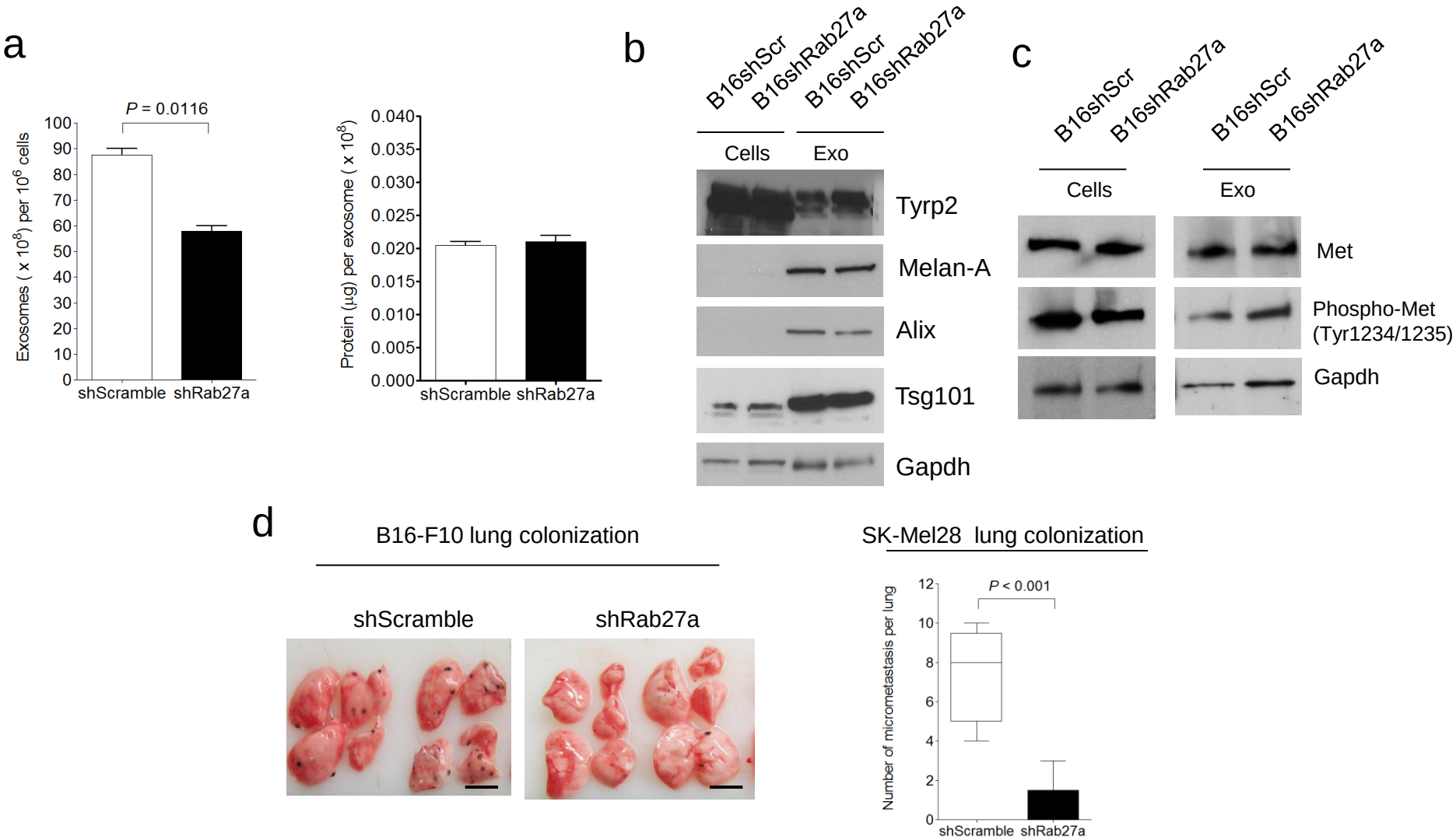

Supplementary Figure 6. Rab27a knockdown reduces exosome release from B16-F10 cells and lung colonization by tumor cells. (a) Analysis of total exosomes secreted by B16-F10shScramble and B16-F10shRab27a cell lines measured by NanoSight (left). The results are presented as the total number of exosomes (× 10^8) per million cells measured by NanoSight. Analysis of total protein per exosome in B16-F10shScramble and B16-F10shRab27a cell lines (right). The results represented as the total micrograms of protein divided by the total number of exosomes (× 10^8) measured by NanoSight. Error bars represent s.e.m. **(b)** Representative western blot analysis of melanoma (Tyrp2, Melan-A) and exosome markers (Alix, Tsg101) in B16-F10shScramble and -shRab27a cell lines (cells) and exosomes (exo). Gapdh was used as loading control. **(c)** Representative Western blot analysis of Met and phospho-Met expression in B16-F10shScramble and -shRab27a cell lines (cells) and exosomes (Exo) **(d)** Analysis of metastasis following shScramble or shRab27a B16-F10 (left) or SK-Mel-28 (right) cell line tail vein injection (see Suppl. methods for details). Gross metastases were macroscopically counted in the lungs of mice injected with B16-F10 cells (black scale bar = 200 mm) and micrometastatic foci in the lung were counted by immunofluorescence ($mCherry^+$) in mice injected with SK-Mel-28 cell models (*n* = 5 mice per group; error bars represent s.e.m).

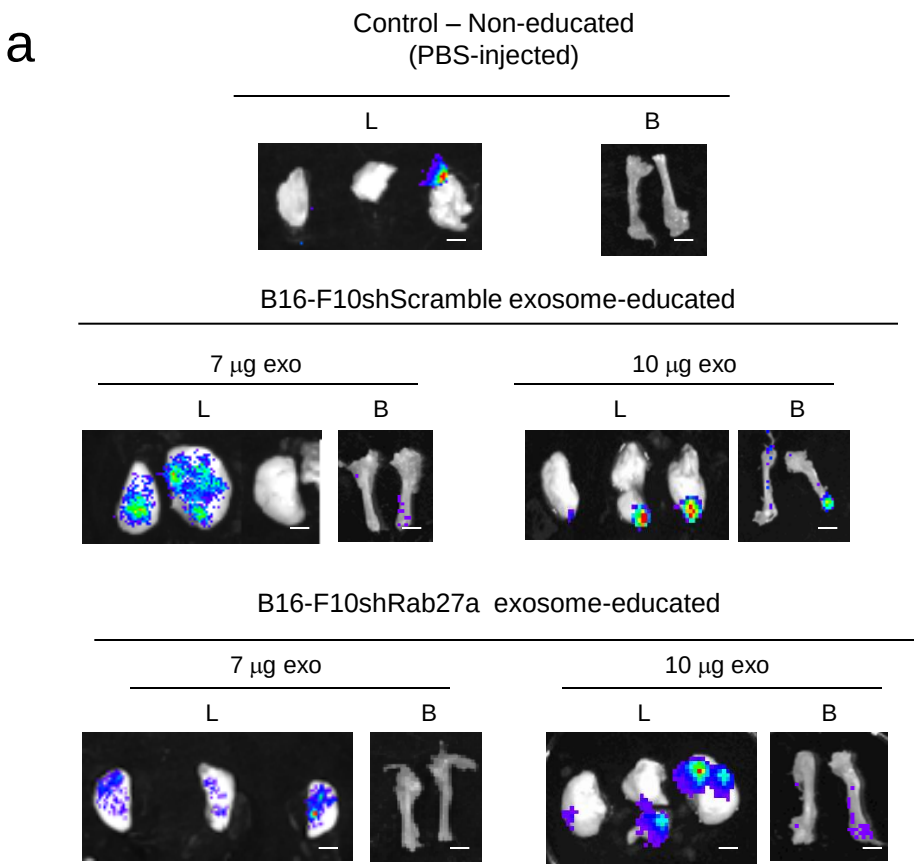

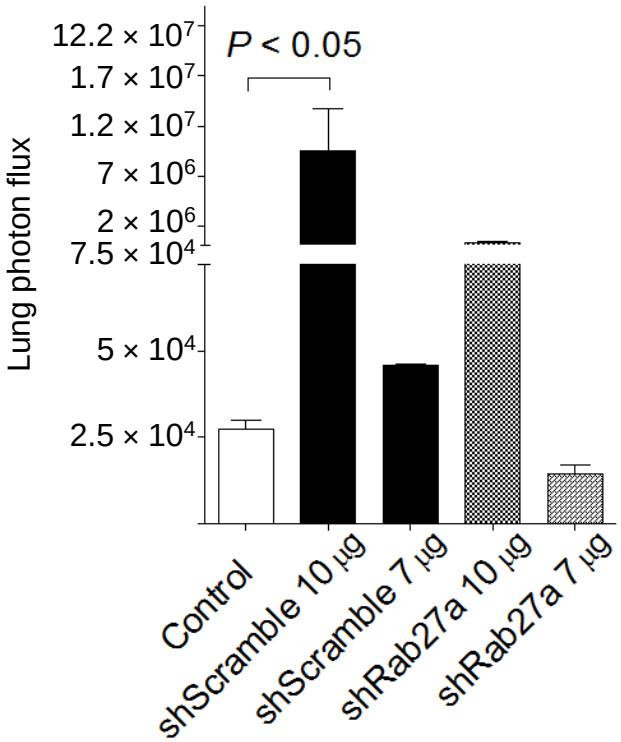

Supplementary Figure 7. Dose response analysis of B16-F10shRab27a exosomes and their influence on metastasis. (a) Analysis of metastases in mice treated with different doses of B16-F10shScramble control exosomes (shScramble 7 and 10μg) and B16-F10shRab27a exosomes (7 and 10 μg). Mice were 'exosome-educated' for 28 d by injecting the indicated dose of exosomes 3 times a week. As controls we used mice injected with PBS following the same schedule. After 28 d of 'exosome education,' 1 x 10^6 B16-F10luciferase cells were injected subcutaneously in the flank of these mice. Metastases were quantified at day 21 post injection (*n* = 5 mice per group, in duplicate). Metastatic lesions were identified by luciferase expression in metastatic organs (lungs (L) and bones (B), scale bar = 200 mm). **(b)** Quantification of total photon flux in lungs. Error bars represent s.e.m.